A Mechanism for the Skew of Ensemble Forecasts

Cécile Penland[1] and Prashant D. Sardeshmukh[2]

[1,2]*NOAA/ESRL/Physical Sciences Laboratory, Boulder, CO*

[2]*Cooperative Institute for Research in Environmental Sciences*,
University of Colorado, Boulder, Colorado.

[1]cecile.penland@noaa.gov

[2]prashant.d.sardeshmukh@noaa.gov

Revised manuscript submitted to *QJRMS*

28 December 2021

Funding provided by the National Oceanic and Atmospheric Administration

Abstract

It is often not appreciated that forecast ensembles are generally skewed. The skew can arise from the state-dependence of the chaotic system dynamics responsible for the ensemble spread. Generation of skew by this mechanism can be demonstrated in even the simplest dynamical system with state-dependent noise, and even when the initial and the asymptotic (that is, the "climatological") forecast distributions are both symmetric. Indeed, forecast distributions of systems with state-dependent noise in the dynamical tendencies must in general be both skewed and heavy-tailed, with implications for forecasting extreme anomaly risks. Ensemble forecast systems that misrepresent such state-dependent noise have state-dependent errors in their forecast probability distributions. Because such errors depend on both the initial condition and forecast lead time, they cannot be removed by simple *a posteriori* bias-corrections of the forecast distributions.

The ensemble standard deviation is often used as a simple metric of ensemble spread even when the forecast distribution is not Gaussian. In a similar spirit, the ensemble skew S may be used as a simple metric of the difference D between the ensemble-mean and most likely forecast as well as the risk ratio R of extreme positive and negative deviations from the ensemble-mean forecast. This is motivated by the facts that 1) the probability distributions of many geophysical quantities are approximately Stochastically Generated Skewed (SGS) distributions, for which simple analytical relationships exist between these quantities, and 2) Gaussian distributions are a sub-class of SGS distributions. However, S may serve as a useful metric of R and D even when the distributions are not strictly SGS distributions.

1. Introduction

A basic feature of weather and climate predictions is their sensitivity to small initial errors. The chaotic nature of earth system dynamics renders accurate deterministic predictions impossible even if the initial errors are tiny.

Operational weather forecasting centers commonly account for forecast uncertainty by providing an ensemble of forecasts generated from an ensemble of slightly different initial conditions, and more recently at some centers, also by stochastically perturbating the forecast model's tendencies at each model time step. It is clear that both initial uncertainties and model uncertainties contribute to forecast uncertainty, and both need to be accounted for to give the best probabilistic forecasts.

Current ensemble forecasting methods yield a crude probability distribution of possible future states, with the ensemble-mean forecast often interpreted as the most likely future state, and the ensemble spread as the forecast uncertainty. For the ensemble to be "reliable" in a probabilistic sense, the actual future state must generally occur within the ensemble spread, that is, the actual forecast uncertainty must be consistent with the expected forecast uncertainty. One measure of this reliability is the consistency between the root-mean-square error of the ensemble-mean forecast determined over many forecast cases and the root-mean-square of the ensemble spread, also determined over many cases. A longstanding problem with most ensemble forecasting systems is that the ensemble spread is generally smaller than the error of the ensemble-mean forecast, that is, the expected forecast uncertainty is too small. This has consequences, especially for predicting extreme event risks.

There are large ongoing efforts in the numerical modeling community to reconcile the forecast error and spread, both by reducing the error and increasing the spread (e.g., Bechtold et al

2008, Leutbecher et al 2017). Efforts to reduce forecast error generally focus on improving the representation of physical processes and increasing the spatial resolution of the forecast model. Efforts to increase forecast spread have traditionally focused on using an ensemble of perturbed initial conditions centered on a more accurately estimated "control" initial condition with special perturbations that grow most rapidly, obtained as either singular vectors or "bred" vectors of the perturbation evolution operator (Molteni et al 1996; Toth and Kalnay 1997). An alternative approach is to use an ensemble of initial states consistent with observational uncertainty, generated using an ensemble data-assimilation algorithm such as an Ensemble Kalman Filter (Evensen 1994). Neither approach has proven effective in eliminating the gap between the forecast error and spread growth with forecast lead time. More recently, some promising results have been obtained by stochastically perturbing the physics and dynamics of the forecast model itself throughout the forecast (Palmer et al 2009, Berner et al 2009, Leutbecher at al 2017, Palmer 2019). Forecast improvements due to such "stochastic parameterizations" are also generally consistent with those obtained by increasing model resolution (Berner et al. 2012, 2017).

Stochastic perturbations are usually justified as accounting for chaotic feedbacks from unresolved model physics and dynamics that are not represented by deterministic parameterizations. Nonlinear interactions, including "deterministic' interactions, that occur on multiple timescales are often described well by a stochastic dynamic "forcing" even when they are generated internally. For example, individual molecular collisions act as state-dependent noise in macroscopic fluid dynamics (Landau and Lifshitz 1959; see García and Penland 1991 for numerical verification). The existence of chaotic interactions at all scales in the geophysical system ensures that stochasticity from various sources is an important contributor to variability in weather and climate. The rich literature showing this to be true has been explored in texts edited by, e.g., Imkeller and Von Storch (2001) and Palmer and Williams (2010), as well as in classic studies such as that of Hasselmann (1976). The discussion in Gottwald (2021) is particularly interesting for its practical advice on how to ensure consistency with pertinent limit theorems in implementing dynamically-based stochastic parameterizations.

Accurate forecasting requires accurate representation of both the resolved aspects of the physical system and the interactions between resolved and unresolved processes. Simply throwing in random numbers to increase the ensemble spread with no regard for the particular physical processes they represent must have limited advantage, although even this is apparently effective in improving estimates of forecast uncertainty (Buizza et al 1999).

Meaningful representation of stochastic effects in a multiscale system must also account for the degree of timescale separation between resolved and unresolved processes. If their separation, defined as the ratio of their autocorrelation timescales, is “infinite”, the stochastic effects may be represented rigorously as a forcing of the resolved scales by a Gaussian white noise forcing with vanishing temporal autocorrelation scales (e.g., Khas’minskii 1966; Papanicolaou and Kohler 1974; Hasselmann 1976). If the separation is large but finite, one may employ a noise forcing with “memory”, such as a Gaussian Ornstein-Uhlenbeck (red noise) forcing with small but finite temporal autocorrelation scales. If the separation does not allow for a complete decoupling of resolved and unresolved timescales, such as when the amplitude of the unresolved processes depends on the amplitude of the resolved processes, one may represent the unresolved chaotic feedbacks on the resolved scales as a state-dependent stochastic forcing. In the simplest case of an energy-conserving system with slow (“resolved”) and fast (“unresolved”) system components, one can rigorously show that such a stochastic coupling yields a *Stochastically Generated Skewed* (SGS) probability distribution of the slow variables (Sardeshmukh and Penland 2015), which in the limit of zero coupling reduces to a Gaussian distribution. Unfortunately, this is where analytical tractability of a smooth transition from a white noise stochastic forcing to a more complex stochastic forcing ends. At the next level of complexity, the chaotic nonlinear resolved-unresolved interactions generally cannot be treated as a linear stochastic process, and the particular forms of the nonlinear terms in a forecast model's equations become important.

Our purpose here is to highlight the fact that forecast ensembles in systems with state-dependent noise are generally skewed, and that the ensemble standard deviation alone does not provide a reliable quantification of forecast uncertainty. The skew strongly affects forecasts of extreme anomaly risks, but is rarely discussed in the forecasting literature (see e.g., overview articles by Leutbecher and Palmer 2008, Palmer 2012, Gneiting and Katzfuss 2014, Leutbecher et al 2017). We stress that the skew due to state-dependent noise is a fundamental property of multi-scale systems with slow and fast components (Sardeshmukh and Penland 2015), and should be distinguished from the skew generated in forecast ensembles by errors in initial conditions and in the deterministic forecast dynamics, such as errors in propagating waves and fronts (e.g. Miller and Ehret 2002, Miyazawa et al 2005, Hodyss and Reineke 2013, Schulte and Georgas 2018).

We investigate the conditional (that is, the forecast ensemble) skew rigorously in the simplest dynamical system with state-dependent noise, specifically a linear scalar system with SGS dynamics, assuming that its sensitivity to initial conditions and forecast lead times will also be illustrative of more complex systems. We do of course recognize that skewness in forecast ensembles can also be generated by deterministic nonlinear processes, not just by state-dependent stochastic processes, and errors in modeling deterministic nonlinear processes as well as observational errors might present additional sources of skew. However, even eliminating such errors would not eliminate the skew in forecast ensembles generated by state-dependent stochastic processes, and we focus on this unavoidable, dynamically-based skew in a simple setting. Further, Sardeshmukh et al (2015) and Sardeshmukh and Sura (2009) provide strong evidence that state-dependent stochastic noise accounts for some basic features of observed large-scale atmospheric non-Gaussianity that are otherwise hard to explain. For example, Sardeshmukh et al. (2015, see their Figs. 2 and 3) used the long-term Twentieth Century Reanalysis dataset to show that for several important meteorological variables, the skew of their probability distributions, the distinctive relationship between the skew and kurtosis, and the approximate equality of their probability densities at standardized positive and negative anomaly magnitudes of $\sqrt{3}$ are all consistent with state-dependent stochastic noise. SGS dynamics may therefore be considered an important generation mechanism for atmospheric non-Gaussianity.

In general, the conditional skew S is associated with a difference D between the ensemble-mean forecast (that is, the mean of the forecast distribution for any desired lead time) and the most likely forecast (the mode of the distribution for that lead time). S is also associated with the risk ratio R of extreme positive and negative deviations from the ensemble-mean forecast being different from unity. Less intuitively but no less importantly, S can also cause the rank histograms of ensemble forecasts determined over many forecast cases (sometimes referred to as Talagrand diagrams), which should ideally be flat, to have a *symmetric* U shape. Such histograms are often used to assess forecast reliability (but see Hamill 2001 for a critique). Their U-shape, an undesirable feature of many ensemble forecast systems, is interpreted as a general underprediction of extreme anomalies and is almost always ascribed to a deficiency in the ensemble spread, not in the ensemble skew. The numerical experiments presented here provide a perspective on how large such effects of S are likely to be in real forecasting contexts for them to matter.

A rigorous characterization of D and R is possible when their underlying stochastic generator is known. Here we exploit the fact that the probability distributions of many large-scale meteorological variables are approximately SGS distributions (e.g., Sardeshmukh et al. 2015; Sardeshmukh and Sura 2009). Such distributions are generated by a combination of correlated additive (that is, the state-independent) and multiplicative (that is, the linearly state-dependent) noise forcing, often referred to as CAM-noise forcing. To distinguish the impact of the stochastic forcing on the forecast spread from that of initial uncertainty, we focus on situations in which the initial conditions are perfect, i.e., δ-functions. Note that the SGS process, being linear, may superpose an ensemble of δ-function initial conditions to describe the results of the whole.

Note also that our focus here is on the skew of the forecast *pdf*, not on the nonlinear evolution of the ensemble-mean forecast *per se*. The ensemble spread and skew are, almost by definition, due to chaotic system dynamics. Our approach of approximating the chaotic dynamics as state-dependent stochastic noise in the simplest model consistent with observed non-Gaussian atmospheric statistics is consistent with the representation of nonlinear chaotic physics by "SPPT" types of stochastic noise parameterizations employed in several state-of-the-art NWP models, and indeed we have found in ongoing research (Sardeshmukh et al 2022, manuscript in preparation) that even our scalar model is useful for understanding the impact of such stochastic parameterizations on forecast skill in the NOAA/GFS model (Wang et al 2019).

We also recognize that there are important meteorological variables whose distributions are not SGS distributions. Because SGS distributions fit the data much better than Gaussian distributions (Sardeshmukh et al 2015), we submit that the skew S of a forecast ensemble is a useful metric of both D and R even when the distributions are only approximately SGS distributions, given the simple relationships between S, D, and R in CAM-noise driven systems.

We submit this noting that the standard deviation of a forecast ensemble is a useful metric of forecast uncertainty even when the distribution is not Gaussian.

The article is arranged as follows. We review the SGS distribution in section 2, summarizing the connection of its parent stochastic differential equation to a nonlinear stochastically forced oscillator, recalling the properties of the unconditional (that is, the stationary) distribution, and revisiting evidence that many important large-scale meteorological variables obey the SGS distribution. In section 3, we note that the conditional (that is, the forecast) probability distribution associated with the stochastic dynamical system obeys the same Fokker-Planck equation obeyed by the stationary distribution, and use it to derive its first four moments for a single initial condition. We numerically generate a large ensemble of realizations of the dynamical system with this initial condition and different realizations of the stochastic noise during system integration. We then repeat these numerical integrations with other initial conditions. The ensemble members from all such integrations are then used to analyze the forecast probabilities as a function of initial condition and forecast lead time. The results presented in sections 3 are based on very large 50000-member ensemble integrations of this simple system, performed to check both numerical accuracy and consistency with theoretical expectations. We also investigate the sampling uncertainties that arise if much smaller but more realistic (100 or 200 member) ensembles sizes are used. Section 4 provides a summary and concluding remarks.

2. Review of SGS dynamics

The SGS distribution was introduced (Sardeshmukh and Sura 2009) as a way to reconcile the observed non-Gaussianity of weather and climate variations with their approximately linear predictability and linear response to external forcing. The linear predictability is evident in many contexts, such as the predictability of tropical SSTs (e.g., Penland and Sardeshmukh 1995, hereafter PS95; Newman and Sardeshmukh 2017). Using Linear Inverse Modeling (LIM) to estimate the SST evolution operator from observed lag-covariances, PS95 found that the results did not seem to depend on the training lag used for the estimation (see also Shin et al 2010). That is, their so-called "tau-test" for linearity was passed. Such a result indicates linear dynamics, almost by definition. However, although seasonally-averaged SSTs are close to Gaussian, monthly averaged SSTs are distributed with significant skew (e.g., Martinez-Villalobos et al 2019), which appears to require nonlinear dynamics. These apparently opposite conclusions regarding linearity can be reconciled if a linear process is driven by correlated additive and multiplicative stochastic noise (CAM noise), which occurs naturally in even very simple multivariate nonlinear systems with slow and fast variables such as a two-dimensional nonlinear oscillator (Sardeshmukh and Penland 2015). The resulting equation for the slow process $x(t)$, adjusted to have zero-mean, is

$$\frac{dx}{dt} = Lx + (Ex + g)\xi_1 + b\xi_2 - \frac{1}{2}Eg. \qquad (1)$$

In Eq. (1), ξ_1 and ξ_2 are independent Gaussian white noises (to be integrated in the sense of Stratonovich), while L, E, g, and b are constants. The stationary, that is the climatological, probability density function (*pdf*: $p(x)$) is evaluated from the stationary Fokker-Planck equation (see Appendix A) as

$$p(x) = \frac{1}{N}[(Ex + g)^2 + b^2]^{-(\nu+1)} \exp\left[q \arctan\left(\frac{Ex+g}{b}\right)\right] \quad , \qquad (2)$$

where $\nu = -[(L / E^2) + 1/2]$, $q = 2g\nu / b$, and N is the normalization constant. Note that ν is constrained to be strictly positive for $p(x)$ to exist, and a necessary condition for the n^{th} moment $<x^n>$ to exist is that $2\nu > (n - 1)$. Further, since the arctangent is bounded and constant for large $|x|$, $p(x)$ has power law tails, with the *pdf* varying as $x^{-2(\nu+1)}$ for large $|x|$.

The multiplicative noise $Ex\xi_1$ and additive noise $g\xi_1 + b\xi_2$ are uncorrelated if $g = 0$. However, when the physical processes represented by these noises are correlated, $g \neq 0$, and cause the stationary *pdf* to be skewed, basically because the magnitude of $Ex + g$ is different for positive and negative x. The stationary mean of x is zero by construction, but the peak of the probability distribution, the mode, is at $x_p = E\,g/(L - E^2/2)$. In fact, since the deterministic parameter L can be absorbed in ν, it is possible to factor L completely out of Eq. (2), and thus out of the location of the mode of the stationary *pdf*, by rescaling E^2, g, and b^2 by the decay rate λ of the lagged autocorrelation of x (see Eq. A4, and Sardeshmukh et al. 2015).

There are other specific properties of $p(x)$ and relationships between moments when $g \neq 0$, which have been used in previous publications (Sardeshmukh and Sura 2009; Sardeshmukh et al. 2015) as strong evidence that the unconditional (that is, the climatological) probability distributions of daily anomalies of important meteorological variables are approximately SGS distributions. Sardeshmukh and Sura (2009) justified the relevance of the SGS distribution associated with a univariate CAM-noise process Eq. (1) in the obviously multivariate real atmospheric system by invoking a principle of "diagonal dominance" in the equations for the higher statistical moments (such as skew, kurtosis, and higher moments) in multivariate linear systems. More rigorously, Sardeshmukh and Penland (2022, manuscript in progress) have recently shown the SGS distribution to be the unconditional distribution of any single component, or any linear combination of components, of a multivariate linear system governed by a vector form of Eq. (1) with multivariate CAM noise forcing.

In this paper we are not so concerned with the unconditional as with the conditional distribution. In a forecasting context, by conditional distribution we mean a distribution conditioned on an initial condition, that one would obtain if the initial condition were perfect or very nearly perfect. Such a distribution would have a finite spread at any forecast lead time because of the chaotic system dynamics. To highlight the general skewness of such conditional distributions, we consider ensemble forecasts from perfect initial conditions in a simple system in which $g = 0$ in the generating equation and the climatological *pdf* is symmetric. As we shall see, the multiplicative noise interacts with any nonzero initial condition in even such a system to generate a conditional skew that reaches a maximum and then decays to zero with forecast lead time.

3. Conditional SGS

Conditional *pdf*s obey the same Fokker-Planck equation that stationary *pdfs* do, except their time derivative in the equation is not zero. Also, in general the normalization constant in the formula for the conditional *pdf* is time-dependent. This is a serious complication in deriving analytical expressions for conditional *pdfs* in CAM-noise driven systems, and indeed we have not derived them. We have, however, derived analytical expressions for their statistical moments in Appendix A. As shown below, our numerical results match these analytical expressions within sampling uncertainty, and the *pdfs* themselves also appear to be SGS *pdfs*, albeit with parameters conditioned on the initial condition.

To demonstrate the general skewness of conditional *pdfs* in even the simplest multiplicative noise driven systems, we numerically generated ensembles of a version of Eq. (1) with $g = 0$. The other parameters were chosen so that the resulting time series $x(t)$ had unit variance and its autocorrelation function decayed exponentially with decay rate $\lambda = 1$. Henceforth, all values of x are presented in units of the climatological standard deviation, and time in units of the decay time $1/\lambda$. Specific values of the parameters are $L = -1.125$, $E^2 = 0.25$, and $b^2 = 1.75$. Each member of an ensemble was integrated from the same initial condition x_o, i.e., $p(x,\ t = 0) = \delta(x - x_o)$. The different members resulted from differed seeds provided to the random number generator returning different time series of ξ_1 and ξ_2.

An ensemble of 50000 members was generated for each initial condition. Each member was integrated using a stochastic fourth-order Runge-Kutta (RK4) scheme (Rümelin 1982). A Mersenne Twister was used to provide random deviates from a uniform distribution, which were then converted to Gaussian deviates using a Box-Müller scheme. The RK4 scheme has been shown to give results consistent with a Stratonovich Mil'steyn scheme (e.g., Kloeden and Platen 1992), and the two schemes have the same formal order of accuracy. Nonetheless, we chose to use the RK4 scheme since it is favored by many scientists.

The number of ensemble members (50000) is much larger than can be reasonably expected of either operational or most research ensemble calculations. We chose such a large ensemble size for our control ensemble to verify our analytical results without seriously having to consider sampling uncertainty. Of course, sampling uncertainty is an important issue in real forecasts. We investigated it by subdividing our 50000-member ensemble into 500 100-member and 250 200-member ensembles and recomputing the results using these smaller and more reasonable ensembles sizes.

We monitored the forecast ensemble histograms for integrations from initial conditions x_o = 1, 3, and 5. Results for the control ensemble using $x_o = 5$ are shown in **Fig. 1*a*** at forecast lead times τ = 0.25, 1, and 7, starting from the delta function at x_o. For reference, we also show the Gaussian histograms (Fig. 1b) obtained from similar ensemble integrations of an Ornstein-Uhlenbeck process, i.e. with both E and g set equal to 0 in Eq. (1) and with L and b^2 adjusted to give unit variance and unit decay time. All histograms were smoothed with a 5-point smoother.

Figure 1 shows that in both the SGS and Gaussian cases the delta-function initial condition evolves into a symmetric stationary *pdf* at long lead times. Note that the mean of the conditional *pdf* (that is, the ensemble-mean forecast) is the same in the two cases at all forecast lead times. However, unlike the Gaussian case, the conditional *pdfs* in the SGS case are skewed and heavy-tailed, and for this initial condition, wider than even the stationary *pdf* !

As shown in Appendix A, the conditional moments can be evaluated using an equation such as Eq.(A6) derived from the Fokker-Planck equation. Solving this equation analytically for the conditional first, second, third, and fourth moments allows evaluation of the conditional variance, skew, and excess kurtosis which can then be compared with the corresponding quantities estimated directly from the forecast ensembles. (Note that unlike the stationary moments, analytical evaluation of these conditional moments does require knowledge of the decay rate, which in our examples is unity). This comparison is shown in **Fig. 2** for the control ensemble as a function of forecast lead time τ for the three initial conditions x_o. To assess the robustness of the numerical results with respect to sampling uncertainty, which can be an issue in estimating higher moments, we also show the analytical and empirical skew and excess kurtosis obtained in the control ensemble integrations from negative mirror initial conditions, $x_o = -1$, -3, and -5. The numerical conditional skew curves for the positive and negative initial conditions are nearly mirror images of one another, as expected, and in excellent agreement with the analytical curves. The agreement of the conditional excess kurtosis curves is however not as good, even using such a large ensemble. Note that in all cases the maximum skew occurs fairly early in the forecasts, at lead times τ between 0.7 and 1.0 decay times.

In the following, we will introduce approximations that rely more on the skew than the excess kurtosis since the skew is more accurately estimated than the kurtosis. In fact, the sample histograms of all conditional moments, including variance, from the 250 sets of 200-member ensembles and from the 500 sets of 100-member ensembles are themselves visibly skewed, and this skew increases with the order of the moment. For this reason, we show median values as well as the 10% confidence levels of the conditional skew as estimated from sets of 100-member and 200-member ensembles in **Fig. 3**. That is, 90% (450 values) of the sample skew**s** estimated from the 100-member ensembles lie above the dotted red line in **Fig. 3.** Thus, the uncertainties in sample skew are large, but not so large as to render the skew unusable. Not surprisingly, estimates of kurtosis using even the larger 200-member ensembles are unreliable.

Since the conditional *pdf*s in a system with a stationary Gaussian *pdf* are Gaussian, the question arises whether conditional *pdf*s in a system with a stationary SGS *pdf* are also SGS *pdfs*. To address this, we used the conditional moments (variance, skew, and excess kurtosis) in our numerical ensembles to estimate the conditional parameters E, g, and b, assuming that they are related to the conditional moments in the same way as the stationary parameters are related to the stationary moments in Eq.(A4). **Fig. 4** shows the parameters estimated from the control ensemble for three initial conditions, $x_o = 1$, 3 and 5, as a function of forecast lead time τ. (In practice, we suggest fitting the conditional *pdfs* using a more robust technique, like the maximum likelihood method or a Bayesian procedure (Bianucci and Mannella 2021), than the "method of moments" used here). The conditional parameters estimated from the control ensemble were then specified in Eq.(A2) to determine candidate conditional SGS *pdfs*. **Fig. 5** shows that these candidate conditional distributions are nearly identical to the histograms obtained from the forecast ensembles for the three initial conditions at unit forecast lead time. We have performed similar comparisons for the other lead times and find agreement between histograms and analytically-fit *pdf*s in all cases. Thus, although we have not been able to show analytically that the conditional *pdf*s are SGS *pdfs*, it is clear that SGS *pdfs* are at least an excellent approximation to the conditional *pdf*s. We are also encouraged to find that these distributions appear to depend only weakly on the kurtosis, since the kurtosis is generally poorly sampled (Fig. 2*d*).

The generation of skew in the forecast ensemble by multiplicative noise results in a difference D between the mean and mode of the conditional *pdfs*. This difference, that we call the forecast distributional bias, is related to the skew S and the multiplicative noise parameter E of the conditional *pdf* as

$$D = x_{mean} - x_{mode} = \frac{\sigma_f}{2}\left(\frac{\lambda - E^2}{\lambda + E^2}\right) S \approx \frac{\sigma_f}{2}\left(\frac{n-3}{n+1}\right) S, \qquad (3)$$

where σ_f is the standard deviation of the conditional *pdf*, and the last approximation follows from assuming that $E^2 \approx 2\lambda/(n-1)$ if the highest moment of $(x - x_{mean})$ that exists is $\langle (x - x_{mean})^n \rangle$. **Fig. 6** shows D estimated from the 100- and 200-member ensembles, but assuming an accurate estimation of E^2, in units of the *stationary* standard deviation σ to facilitate intercomparison among the different forecast cases. Like the conditional moments, the distribution of sampled D is skewed. Dotted lines indicate the 10% confidence level, meaning that 90% of the sample D values lie above these curves. Also shown are values of D using parameters estimated from the theoretical moments derived in Appendix A. For all three initial conditions x_o, D peaks at lags of about $\tau = 0.6$ but remains large for longer lead times. Not surprisingly, D is largest for forecasts from $x_o = 5$, since the multiplicative noise is relatively largest in that case, but D generally cannot be ignored even in the case of the much less extreme initial condition $x_o = 1$; the median (50% confidence level) values of D are close to the theoretically estimated values.

The skew of the forecast ensemble also affects the predicted risk ratio R of extreme positive and negative deviations from the ensemble-mean forecast. For simplicity, we define these extremes as ± 2 standard deviations from the ensemble-mean forecast. That is, for $\tilde{x} = (x - x_{mean})/\sigma_f$, where x_{mean} and σ_f are the mean and standard deviation of the conditional *pdf*, respectively, we define $R = p(\tilde{x} = +2)/p(\tilde{x} = -2)$. Fig. 7 shows R as a function of forecast lead time for the three initial conditions x_o using Eq. 2 and parameters estimated from the control ensemble with 50000 members (black circles; see Fig. 5). Note that in the Gaussian (Ornstein-Uhlenbeck) case, $R = 1$ at all lead times. In the SGS case, R is clearly not equal to 1, and for small S, is related approximately to S as

$$R \approx exp\left[S\,\frac{\tilde{x}\,(\tilde{x}^2-3)}{3}\right] = exp\left[\frac{2}{3}S\right]. \qquad (4)$$

We tested this simple approximation to R using our 100- and 200-member ensembles. **Fig. 7** shows that the approximation appears to be valid for conditionals skews smaller than about 0.5. As with the conditional moments and D, the distributions of R estimated from our ensemble sets are skewed. In all cases, the values of R estimated from the *pdf*s shown in Fig. 5 are well within the range of ensemble values.

5. Discussion and Concluding Remarks

We have argued that forecast ensembles in the climate system must be generally skewed, in part because the chaotic system dynamics responsible for the ensemble spread are generally state dependent. We showed that forecast ensembles are skewed even in the simplest scalar linear dynamical system with state-dependent noise, and even when the initial and the long-lag ("climatological") ensembles are not skewed. The ensemble skew S is related to two other important aspects of ensemble asymmetry: the difference D between the expected mean and most likely forecast, and the risk ratio R of extreme positive and negative deviations from the ensemble-mean forecast. In our simple system, which has relevance in weather and climate dynamics (e.g., Sardeshmukh et al. 2015), these relationships can be made explicit. This motivates us to propose S as a generally useful metric of ensemble forecast information, in addition to the ensemble mean and spread.

State-dependent (multiplicative) and state-independent (additive) noises can both increase forecast spread. Unlike additive noise, however, multiplicative noise can make the spread even larger than the climatological standard deviation and generate skewed and heavy tailed forecast distributions. These effects can cause predictions of extreme anomaly risks to strongly differ from similar forecasts based on Gaussian statistics.

In our illustrative examples, the multiplicative noise effects on the forecast *pdfs* peaked at forecast lead times $\tau \sim 1$, and were relatively large when the initial anomaly was large ($x_o = 5$). The basic reason for this is not hard to understand. When the initial anomaly is large, the multiplicative noise is also relatively large, and can push the system to even larger values than additive noise. The effect becomes smaller after $\tau \sim 1$ in all forecast cases as the ensemble drifts towards climatology and x becomes smaller.

Analysis of a multivariate CAM-noise system (Sardeshmukh and Penland 2022, manuscript in progress) suggests that one may reasonably assume results from this simple system to be generally relevant even in multi-dimensional systems with state-dependent noise. Further, Thompson et al. (2017) have shown that homogenization of a system driven by linear CAM noise rigorously converges to one driven by an α-stable Lévy process, whose self-similar properties of the *pdf* are well-known. If the CAM noise process were to be far from self-similar itself, one would not expect it to be such a good approximation of a Lévy process as it is (Penland and Sardeshmukh 2012; Gottwald 2021).

The fact that the largest multiplicative noise effects occur for forecasts from extreme initial conditions highlights the importance of properly accounting for them in predictions of extreme events. We should note that in a multi-component system such extreme initial conditions need not be associated with extremely large-amplitude initial anomaly vectors as in our scalar 1-component system, but merely have a large projection on the optimal initial vectors for anomaly growth over the global forecast domain or a desired sub-domain. Such optimal vectors, usually identified with the dominant singular vectors (SVs) of the system's perturbation evolution operator, have found extensive application in initial ensemble design and predictions (e.g., Buizza and Palmer 1995). Multiplicative noise in the evolution from an initial SV perturbation to an extreme large-amplitude perturbation would then generate large skew in the forecast *pdfs* even from small initial amplitudes in this vector scenario, unlike in the scalar 1-component scenario.

Finally, because multiplicative noise effects on forecast *pdfs* depend on the initial condition as well as forecast lead time, one cannot account for them using state-independent *a-posteriori* probabilistic bias corrections. For example, it may be tempting to correct for the undesirable symmetric U shapes of rank histograms in many ensemble forecasting systems through state-independent adjustments of the ensemble spread. However, in reality such a symmetry may also arise from a conflation of spuriously skewed conditional pdfs in forecasts from positive and negative initial conditions (see Fig 2c), as also noted by Hamill (2001). One may think of addressing such issues by stratifying the *a-posteriori* corrections with respect to initial conditions and forecast lead times. This is possible in principle, but impractical in high dimensional systems. A more practical and physically grounded approach is to attempt to represent such state-dependent noise effects, however crudely, in the forecast model itself through stochastic parameterizations of the state-dependent chaotic model tendencies. As mentioned in the introduction, such approaches have already proven beneficial in operational ensemble forecasting. The analysis of this paper further highlights the need to continue improving such parameterizations to continue improving the prediction and dissemination of extreme anomaly risks.

Acknowledgments: The authors acknowledge useful comments by all of the reviewers. This work was partially funded through NOAA's Weather Prediction Office.

Appendix A

Given Eq. (1), the Stratonovich form of the Fokker-Planck equation for the conditional probability that the system is found between x and $x+dx$ at time t when the initial condition at t=0 is x_O is

$$\frac{\partial p(x,t|x_o)}{\partial t} = -\frac{\partial}{\partial x}\left[\left(L+\tfrac{1}{2}E^2\right)xp(x,t|x_o)\right] + \frac{1}{2}\frac{\partial^2}{\partial x^2}\{[(Ex+g)^2+b^2]p(x,t|x_o)\}. \quad \text{(A1)}$$

This equation is also obeyed by the stationary probability density function (*pdf*) $p(x)$ for x with the time derivative on the left-hand side set to zero. Integrating the equation for the stationary *pdf* once over x and using the fact that $p(x)$ vanishes as x gets infinitely large yields

$$p(x) = \frac{1}{N}[(Ex+g)^2+b^2]^{-(\nu+1)}\exp\left[q\arctan\left(\frac{Ex+g}{b}\right)\right] \quad \text{(A2}a\text{)}$$

where $\nu = -[(L/E^2)+1/2]$, $q = 2g\nu/b$, and N is a normalization constant

$$N = \frac{2\pi}{E}(2b)^{-(2\nu+1)}\frac{\Gamma(2\nu+1)}{\Gamma(\nu+1-iq/2)\Gamma(\nu+1+iq/2)}. \quad \text{(A2}b\text{)}$$

Note that in Eq. (A2) the deterministic parameter L occurs only in terms of ν. It is therefore possible to factor it completely out of the equation. In Sardeshmukh et al. (2015), the parameter $\lambda = -(L+E^2/2)$ was used to rescale E^2, g, and b^2, rendering a three-parameter version of (A2) that is completely equivalent numerically. Note that λ is the rate that the autocorrelation of x decays and is therefore easily estimated from data.

Eq. (1) has been developed for an anomalous state variable so that the stationary mean $<x>$ is zero. As shown in Sardeshmukh et al (2015), the parameters E, g, and b can be estimated from the moments of $p(x)$ in terms of λ. Recalling the general definitions of variance σ^2, skew S, and excess kurtosis K:

$$\sigma^2 = <(x - <x>)^2> \tag{A3a}$$

$$S = <(x - <x>)^3> / \sigma^3 \tag{A3b}$$

$$K = <(x - <x>)^4> / \sigma^4 - 3\ , \tag{A3c}$$

the following expressions for E, g, and b can be derived analytically and evaluated sequentially:

$$E^2 = \left(\frac{2}{3}\right)\frac{\left[K - \frac{3}{2}S^2\right]}{[K - S^2 + 2]}\lambda \tag{A4a}$$

$$g = S\sigma\left(\frac{1 - E^2/\lambda}{2E}\right)\lambda \tag{A4b}$$

$$b^2 = 2\sigma^2\left[1 - \frac{\lambda E^2}{2} - \frac{(1 - \lambda E^2)^2}{8\lambda E^2}S^2\right]\lambda. \tag{A4c}$$

The system considered here has a stationary *pdf* that is symmetric, i.e., $g = 0$. We have shown numerically that even in this case the conditional *pdf* is skewed. However, it is not clear if the conditional probability $p(x,t|x_o)$ is strictly a *Stochastically Generated Skewed* (SGS) distribution of the form (A2). If so, the parameters of $p(x,t|x_o)$ could be estimated from expressions (A3) and (A4), with all of the moments in Eq. (A3), including the means and standard deviations

σ, replaced by the conditional moments. Recall that the conditional probability $p(x, t|x_o)$ obeys the same equation as the stationary probability $p(x)$, retaining the time derivative. For our system, that is

$$\frac{\partial p(x,t|x_o)}{\partial t} = -\frac{\partial}{\partial x}\left[\left(L + \tfrac{1}{2}E^2\right)xp(x,t|x_o)\right] + \frac{1}{2}\frac{\partial^2}{\partial x^2}\{[E^2x^2 + b^2]p(x,t|x_o)\}. \quad \text{(A5)}$$

The time derivative makes it more difficult to solve for $p(x, t\,|x_o)$. However, it is easy to derive solvable equations for the conditional moments via integration by parts. The equation for the n^{th} conditional moment at time $t = \tau$ given an initial condition x_o at $t = 0$ reads

$$\frac{\partial < x^n(\tau)|x_o >}{\partial \tau} = n\left(L + \frac{1}{2}E^2\right) < x^n(\tau)|x_o >$$
$$+ \frac{1}{2}n(n-1)[E^2 < x^n|x_o > + b^2 < x^{n-2}|x_o >] \quad . \quad \text{(A6)}$$

Solving Eq. (A6) for the first four conditional moments in terms of the stationary variance σ^2, and using the fluctuation-dissipation relation to eliminate b, we find

$< x(\tau) \mid x_o > = \exp\,[(L + {}^1/_2E^2)\;\tau]\;x_o$ (A7*a*)

$< x^2(\tau) \mid x_o > = \exp\,[\,2(L + E^2)\,\tau\,]\;x^2_o + (1 - \exp\,[2\,(L + E^2)\,\tau\,])\;\sigma^2$ (A7*b*)

$< x^3(\tau) \mid x_o > = \exp\,[\,3(L + {}^3/_2\,E^2)\,\tau]\;\; x^3_o\; +$

$$\frac{3(L+E^2)}{(L+2E^2)}\,\sigma^2\,(1 - \exp[\,2(L+2E^2)\,\tau\,])\;\exp\,[(L + {}^1/_2E^2)\;\tau\,]\;x_o \quad \text{(A7}c\text{)}$$

$< x^4(\tau) \mid x_o > = \exp\,[\,4(L + 2E^2)\;\tau]\;x^4_o$

$$- 6\frac{(L+E^2)}{(L+3E^2)}\,\sigma^2(\,\sigma^2 - x^2_o\,)\ \exp[2(L+E^2)\ \tau]\ (1 - \exp[2(L+3E^2)\ \tau]$$

$$+ 3\sigma^4\frac{(L+E^2)}{(L+2E^2)}(1 - \exp[\ 4(L + 2E^2)\ \tau]\ ) \quad . \qquad (A7d)$$

Using the conditional moments in Eqs. (A3) and (A4) to estimate the conditional parameters $E^2(x,\tau|x_o)$, $g(x,\tau|x_o)$ and $b^2(x,\tau|x_o)$ in terms of λ, one can evaluate a conditional, unnormalized version of Eq. (A2*a*). Translating x appropriately by $<x \mid x_o>$ and normalizing numerically, we compare the SGS estimation of $p(x,\ \tau \mid x_o)$ with the estimation of $p(x,\ \tau \mid x_o)$ from the raw histogram (Fig. 5). We leave analytical verification of their equivalence to those with more patience and/or better symbolic manipulators than we have. (Such hardy souls would have to contend with Gamma functions of temporally-varying, complex argument in the normalization factor contributing to the left side of Eq. (A5))

References

Bechtold, P., Koehler, M., Jung, T., Doblas-Reyes, F.J., Leutbecher, M., Rodwell, M.J.,) Vitart, F., and G. Balsamo, 2008: Advances in simulating atmospheric variability with the ECMWF model: From synoptic to decadal time-scale**s.** *Quarterly Journal of the Royal Meteorological Society*, 134, 634, 1337-1351, Part A. doi: 10.1002/qj.289

Berner J, Shutts GJ, Leutbecher M, Palmer TN. 2009. A spectral stochastic kinetic energy backscatter scheme and its impact on flow-dependent predictability in the ECMWF ensemble prediction system. *J. Atmos. Sci*. 66: 603–626.

Berner, J., Jung, T., and T. N. Palmer, 2012: Systematic model error: The impact of increased horizontal resolution versus improved stochastic and deterministic parameterizations. *J. Climate*, **25**, 4946–4962, doi:10.1175/JCLI-D-11-00297.1.

Berner, J., and Coauthors, 2017: Stochastic parameterization: Toward a new view of weather and climate models. *Bull. Amer. Meteor. Soc.*, 98, 565–588, https://doi.org/10.1175/BAMS-D-15-00268.1.

Bianucci, M., and R. Mannella, 2021: On the determination of the optimal parameters in the CAM model. *Chaos*, **31**, 033113; doi: 10.1063/5.0032267.

Buizza, R., and T.N. Palmer TN. 1995: The singular-vector structure of the atmospheric global circulation. *J. Atmos. Sci*., **52**, 1434-1456.

Buizza, R., Miller, M., and T.N. Palmer TN. 1999: Stochastic representation of model uncertainties in the ECMWF ensemble prediction system. *Q. J. R. Meteorol. Soc*. 125: 2887–2908.

Compo, G.P, and Coauthors, 2011: The Twentieth Century Reanalysis Project. Quart. J. Roy. Meteor. Soc., 137, 1–28, doi:10.1002/qj.776.

Evensen, G., 1994: Sequential data assimilation with a nonlinear quasi-geostrophic model using Monte-Carlo methods to forecast error statistics. *J. Geophys. Res.,***99** (C5), 10143–10162.

García, A., and C. Penland, 1991: Fluctuating hydrodynamics and Principal Oscillation Pattern analysis. *J. Stat. Phys.*, **64**, 1121-1132.

Gneiting, T., and M. Katzfuss, 2014: Probabilistic forecasting *Annu. Rev. Stat. Appl*., 125-151

Gottwald, G.A. A model for Dansgaard–Oeschger events and millennial-scale abrupt climate change without external forcing. *Clim Dyn* **56,** 227–243 (2021). https://doi.org/10.1007/s00382-020-05476-z

Hamill, T. M., 2001: Interpretation of rank histograms for verifying ensemble forecasts. *Mnthly Weath. Rev.,* 129, 550–560.

Hasselmann, K., 1976: Stochastic Climate Models. Part I. Theory. *Tellus*, **28**, 473-485.

Hodyss, D., and A. Reineke, 2013: Skewness of the Prior Through Position Errors and Its Impact on Data Assimilation. In S.K. Park and L. Xu (eds.), *Data Assimilation for Atmospheric, Oceanic and Hydrologic Applications* (Vol. II), DOI 10.1007/978-3-642-35088-7 7.

Imkeller, P., and J.-S. von Storch, 2001: *Stochastic Climate Models*, Birkäuser, Basel.

Khas'minskii, R. Z., 1966: A limit theorem for the solutions of differential equations with random right-hand sides. *Theory Probab. Appl.*, **11**, 390–406, doi:10.1137/1111038.

Kloeden, P. E., and E. Platen, 1992: *Numerical Solution of Stochastic Differential Equations*. Springer-Verlag, 632 pp.

Landau, L.D., and E.M. Lifschitz, 1959: *Fluid Mechanics*, Pergamon Press, Oxford.

Leutbecher, M., and T.N. Palmer, 2008: Ensemble forecasting. *Journal of Computational Physics*, 227, 3515–3539. https://doi.org/10.1016/j.jcp.2007.02.014.

Leutbecher, M., Lock, S.J., Ollinaho, P., Lang, S.T.K., Balsamo, G., Bechtold, P., Bonavita, M., Christensen, H.M., Diamantakis, M., Dutra, E., English, S., Fisher, M., Forbes, R.M., Goddard, J., Haiden, T., Hogan, R.J., Juricke, S., Lawrence, H.,MacLeod, D.,Magnusson, L.,Malardel, S., Massart, S., Sandu, I., Smolarkiewicz, P.K., Subramanian, A.,Vitart, F.,Wedi,N., and Weisheimer, A. (2017) Stochastic representations of model uncertainties at ECMWF: stateof the art and future vision. *Quarterly Journal of the Royal Meteorological Society*, 143(707), 2315–2339. https://doi.org/10.1002/qj.3094.

Martinez-Villalobos, C., Newman, M., Vimont, D. J., Penland, C., & David Neelin, J. (2019). Observed El Niño-La Niña asymmetry in a linear model. *Geophysical Research Letters*, **46**, 9909–9919. https://doi.org/10.1029/2019GL082922

Molteni, F., , R. Buizza, , T. N. Palmer, , and T. Petroliagis, 1996: The ECMWF ensemble prediction system: Methodology and validation. *Quart. J. Roy Meteor. Soc*, **122 ,** 73–120.

Miller, R.N., and L.L. Ehret, 2002: Ensemble generation for models of multimodal systems. Mon. Wea. Rev., 130, 9, 2313-2333.
DOI: 10.1175/1520-0493(2002)130<2313:EGFMOM>2.0.CO;2

Miyazawa, Y., Yamane, S., Guo, X., and T. Yamagata, 2005: Ensemble forecast of the Kuroshio meandering. J. Geophys. Res, 110, C10026, doi:10.1029/2004JC002426

Newman, M., and P.D. Sardeshmukh, 2017:. Are we near the predictability limit of tropical Indo-Pacific sea surface temperatures? Geophysical Research Letters, 44, 8520–8529. https://doi.org/10.1002/2017GL074088

Palmer, T.N., R. Buizza, F. Doblas-Reyes, T. Jung, M. Leutbecher, G. Shutts, M. Steinheimer, and A. Weisheimer, 2009: Stochastic parametrization and model uncertainty. ECMWF Tech. Memo. 598, 44 pp. [Available online at www.ecmwf.int/sites/default/files/elibrary/2009/11577-stochastic-parametrization-and-model-uncertainty.pdf.]

Palmer, T. N., 2019: Stochastic weather and climate models. *Nat. Rev. Phys.*, 1, 463–471, https://doi.org/10.1038/s42254-019-0062-2.

Palmer, T.N., and P. D. Williams, 2010: *Stochastic Physics and Climate Modelling*. Cambridge University Press, Cambridge, 480pp.

Papanicolaou, G., and W. Kohler, 1974: Asymptotic theory of mixing ordinary stochastic differential equations. *Commun. Pure Appl. Math.*, **27**, 641–668, doi:10.1002/cpa.3160270503.

Penland, C., and P. D. Sardeshmukh, 2012: The optimal growth of tropical sea surface temperature anomalies. J. Climate, 8, 1999–2024.

Penland, C., and P. D. Sardeshmukh, 2012: Alternative interpretations of power-law distributions found in nature. *Chaos*, **22**, 023119, doi:10.1063/1.4706504.

Rüemelin, W., 1982: Numerical treatment of stochastic differential equations. *SIAM J. Numer. Anal.*, **19**, 604–613, doi:10.1137/0719041.

Sardeshmukh, P. D., and P. Sura, 2009: Reconciling non-Gaussian climate statistics with linear dynamics. *J. Climate*, **22**, 1193–1207, doi:10.1175/2008JCLI2358.1.

Sardeshmukh, P.D., and C. Penland, 2015: Understanding the distinctively skewed and heavy tailed character of atmospheric and oceanic probability distributions. *Chaos*, **25**, 036410, doi:10.1063/1.4914169.

Sardeshmukh, P.D., G. P. Compo, and C. Penland, 2015: Need for caution in interpreting extreme weather statistics. *J. Climate*, **28**, 9166–9187, doi:10.1175/JCLI-D-15-0020.1.

Schulte, J., and N. Georgas, 2018: Theory and practice of phase-aware ensemble forecasting. *Quart. J. Royal Met. Soc*., 144, 714, 1415-1428, Part A. DOI: 10.1002/qj.3285

Shin, S. I., Sardeshmukh, P.D., and K. Pegion, 2010: Realism of local and remote feedbacks on tropical sea surface temperatures in climate models. *J. Geophys. Res*., 115, D21110, doi:10.1029/2010JD013927.

Thompson W.F., Kuske R.A., and A.H. Monahan, 2017: Reduced α-stable dynamics for multiple time scale systems forced with correlated additive and multiplicative Gaussian white noise. *Chaos: An Interdisciplinary Journal of Nonlinear Science* 27(11):113105.

Toth, Z., and E. Kalnay, 1997: Ensemble forecasting at NCEP and the breeding method. *Mon. Wea. Rev.,***126,** 3292–3302.

Wang, J.W.A, Sardeshmukh, P.D., Compo, G.P., Whitaker, J.S., Slivinski, L., and P. Pegion, 2019: Sensitivities of the NCEP Global Forecast System. *Mon. Wea. Rev*. 147, 4,1237-1256.

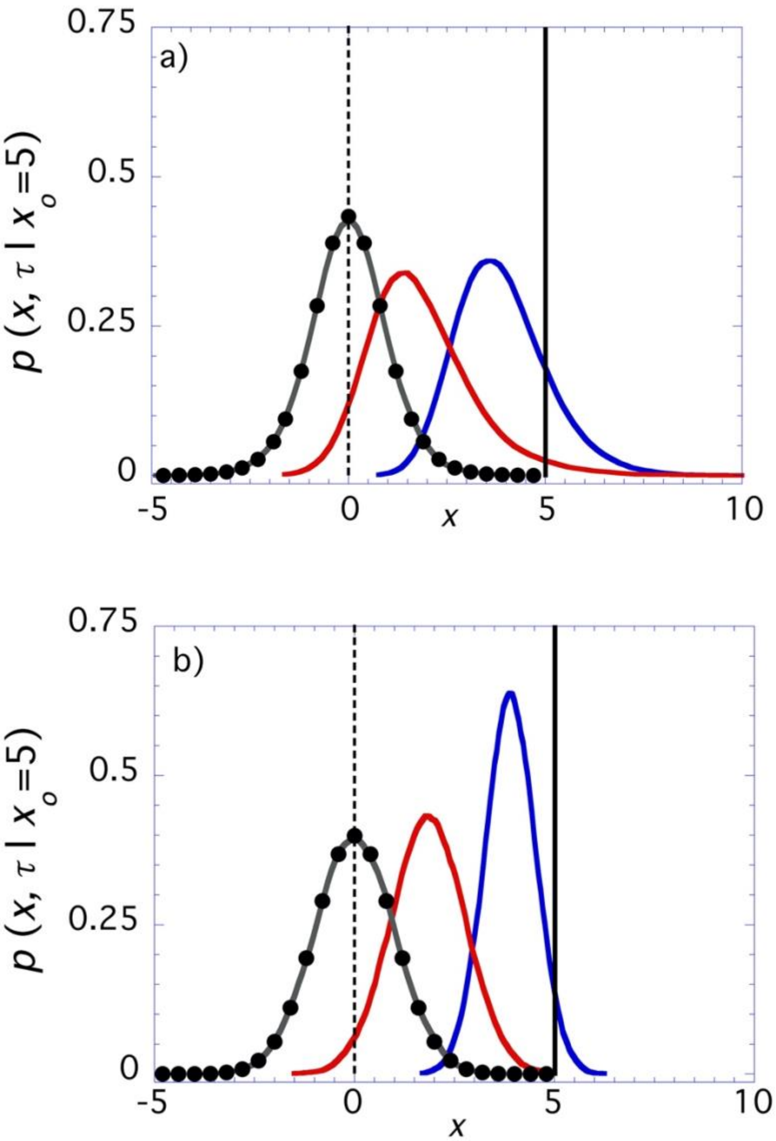

Fig. 1: Snapshots of conditional (forecast) probability density functions (*pdf*s) of ensemble forecasts starting from an initial condition $x_o = 5$ (solid vertical line), at lead times of $\tau = 0.25$ (blue line), 1 (red line), and 7 (black line). Analytical stationary *pdf* is shown with black symbols, and its zero mean as a dotted vertical line. *(a)* Top: Stochastically Generated Skew process. (*b*) Bottom: Ornstein-Uhlenbeck Gaussian process. All distributions have been smoothed with a five-point smoother. Note that the conditional *pdfs* are skewed and heavy tailed in (a) but Gaussian in (b).

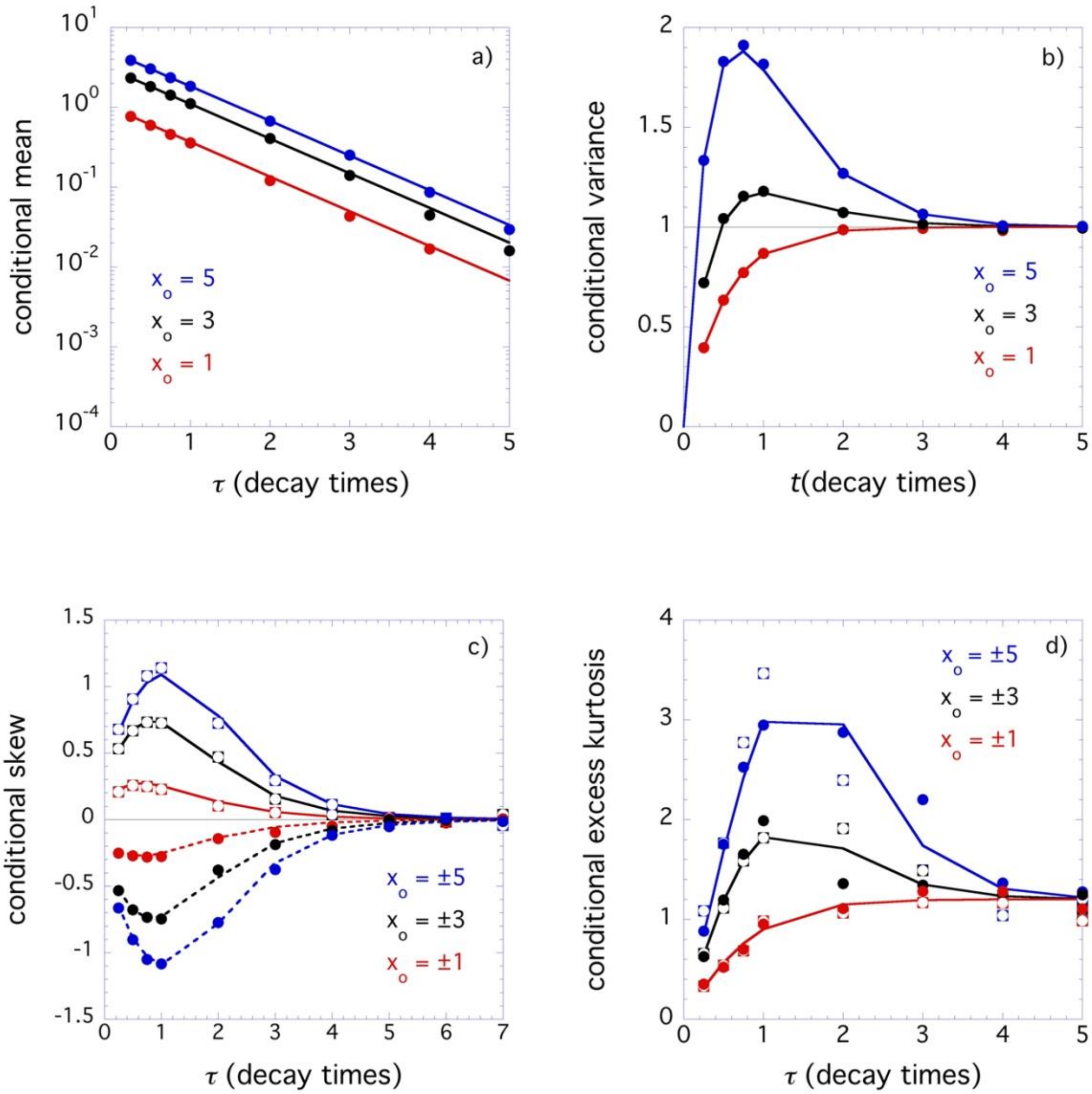

Fig. 2: Conditional moments as a function of forecast lead time. Symbols: Using forecast values from the ensemble members. Lines: Analytical values. *a*) Conditional mean for $x_o = 1$ (red lines), 3 (black lines), and 5 (blue lines). *b*) Same as *a*) but for conditional variance. *c*) Conditional skew for $x_o = 1$, 3, and 5 (open symbols and solid lines) and for $x_o = -1$, -3, and -5 (solid symbols and dotted lines. *d*) Same as *c*) but for conditional excess kurtosis.

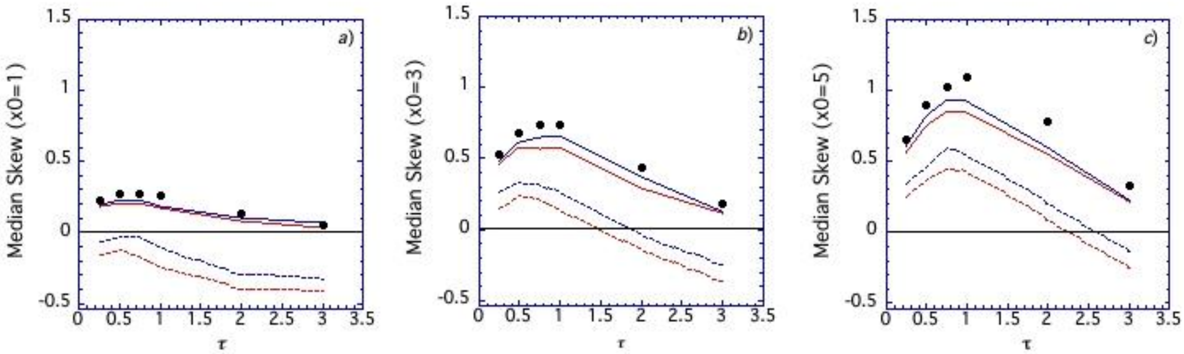

Fig. 3: Sample conditional skew estimated from 500 100-member ensembles (red lines) and 250 200-member ensembles (blue lines) for initial conditions x_o = 1, 3, and 5. Black dots: values estimated from expressions derived in Appendix A. Lines: Median skew of the ensembles. Dotted lines: 10% confidence levels based on number of 100-member (red) and 200-member (blue) ensembles.

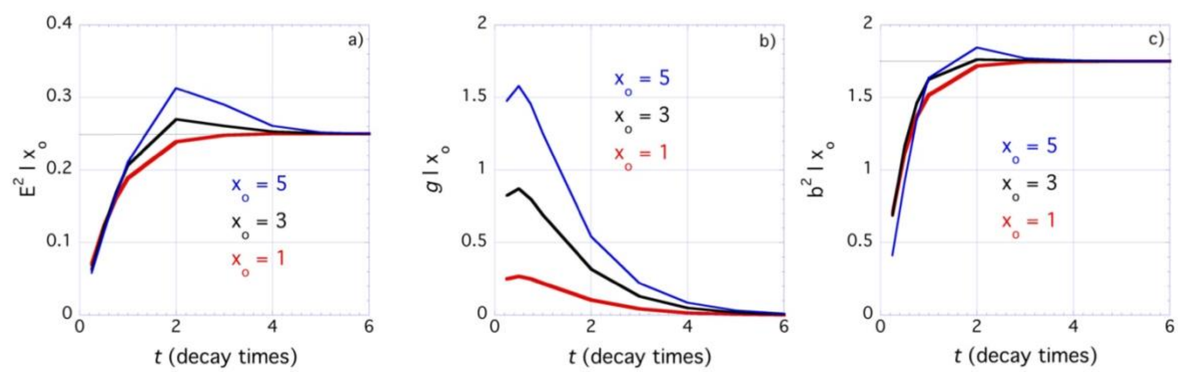

Fig. 4: Conditional SGS parameters as a function of forecast lead time for initial conditions x_o = 1 (red line), 3 (black line), and 5 (blue line). *a*) E^2 given x_o, *b*) g given x_o. *c*) b^2 given x_o. Climatological values are E^2 = 0.25, g = 0., and b^2 = 1.75.

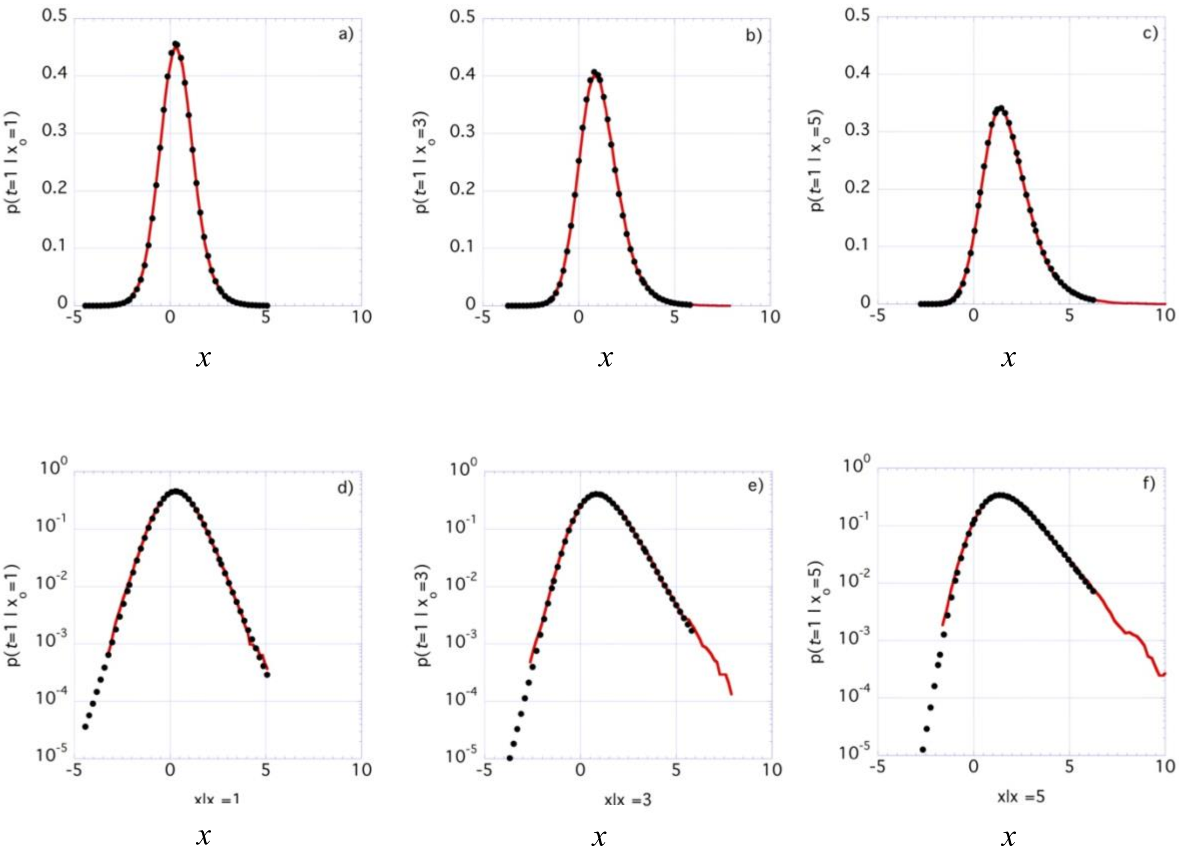

Fig. 5: Conditional probability distribution functions (*pdf*s) at lead time $\tau = 1$ estimated using forecast values from the ensemble members (red lines) and derived analytically using the estimated conditional SGS parameters (black symbols). Top row (*a-c*): For initial conditions x_o = 1, 3, and 5, on a linear scale. Bottom row (*d-f*): As in the top row, but on a logarithmic scale.

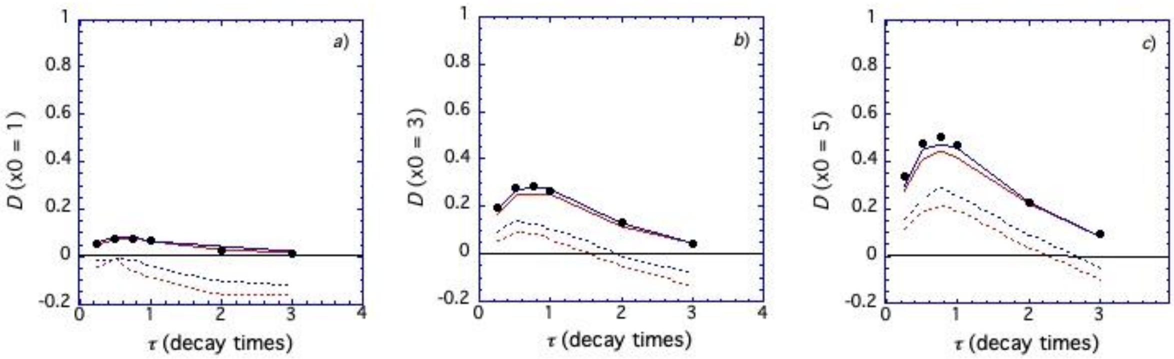

Fig. 6: Distributional bias D, i.e. conditional *pdf* mean minus the *pdf* mode, as a function of lead time for *a)* $x_o = 1$, *b)* $x_o = 3$, and *c)* $x_o = 5$. Solid lines: Eq. (3) median of 500 100-member ensembles (solid red lines) and of 250 200-member ensembles (solid blue lines). Dashed lines: 10% confidence levels. Symbols: Values estimated from Fig. 5 and Fig. 2*a*.

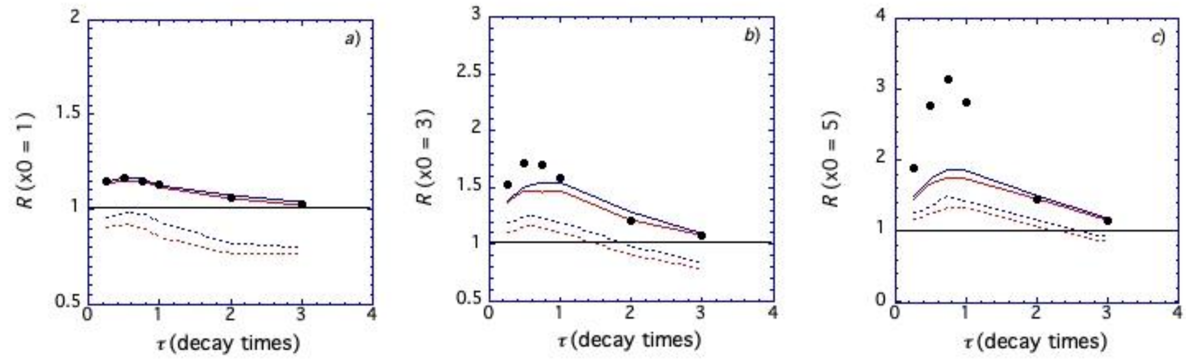

Fig. 7: Conditional risk ratio R defined in Eq. (4) as a function of lead time for *a)* $x_o = 1$, *b)* $x_o = 3$, and *c)* $x_o = 5$. Black circles: Values estimated from *pdf*s shown in Fig. 5. Approximations of R using only skew (Eq. 4) are shown for the 100-member (red lines) and 200-member (blue lines) ensemble sets. Solid Lines: median approximate values of R. Dashed Lines: 10% confidence levels. Accurately estimated quantities (symbols) are well within the range of ensemble values; the 90% confidence levels are off the scale of the graphs.